Prewetting transitions of Ar and Ne on alkali-metal surfaces

Francesco Ancilotto and Flavio Toigo
Istituto Nazionale per la Fisica della Materia and Dipartimento di Fisica G.Galilei, Universita' di Padova, via Marzolo 8, 35131 Padova, Italy
(Received 3 May 1999)

We have studied by means of density-functional calculations the wetting properties of Ar and Ne adsorbed on a plane whose adsorption properties simulate the Li and Na surfaces. We use reliable *ab initio* potentials to model the gas-substrate interactions. Evidence for prewetting transitions is found for all the systems investigated and their wetting phase diagrams are calculated. [S0163-1829(99)01536-2]

I. INTRODUCTION

Direct evidence for the first-order nature of the wetting transition, as originally predicted by Cahn,[1] together with the characteristic prewetting jumps away from the coexistence line, has been obtained in several different systems: quantum liquid films physisorbed on heavy alkali metals,[2] complex organic liquids,[3] near-critical liquid mercury,[4] and binary liquid crystal mixtures.[5,6]

Quite generally, wetting transitions at temperatures above the triple point are expected for weakly attractive substrates. In particular, it was argued that alkali metals provide the weakest adsorption potentials of any surfaces for He atoms and therefore that wetting transitions could be observed on such substrates.[7] This hypothesis has subsequently been confirmed and the corresponding transition studied in many laboratories.[8–10] More recently, similar phenomena have also been predicted and/or seen for H_2, Ne, and Hg on various surfaces.[11–16]

Theory dictates[17,18] that when a first-order transition from partial to complete wetting occurs at a temperature T_w above the triple point (and below the bulk critical temperature), then a locus of first-order surface phase transitions must extend away from the vapor-fluid coexistence curve, on the vapor side. At $T<T_w$ the thickness of the adsorbed liquid film increases continuously with pressure, but the film remains microscopically thin up to the coexistence pressure $P_{sat}(T)$, and becomes infinitely (macroscopically) thick just above it. The adsorption isotherms reach $P_{sat}(T)$ with a finite slope. At temperatures $T_w<T<T_{pw}^c$ (T_{pw}^c being the prewetting critical temperature) the thin film grows as the pressure is increased until a transition pressure $P_{tr}(T)<P_{sat}(T)$ is reached. At this pressure a thin film is in equilibrium with a thicker one, and a jump in coverage occurs as P increases through $P_{tr}(T)$. At still higher pressures this first order transition is followed by a continuous growth of the thick film, which becomes infinitely thick at $P_{sat}(T)$. The discontinuity (i.e., the difference in thickness between the two films in equilibrium) becomes smaller and smaller as T increases above T_w, until at a temperature T_{pw}^c the two films are no longer distinguishable from one another. Finally, when $T>T_{pw}^c$, the adsorbed liquid film increases continuously with pressure to become infinitely thick at $P_{sat}(T)$.

Noble-gas fluids (other than He) adsorbed on weakly attractive substrates such as the surface of alkali metals, are good candidates for showing prewetting transitions. There is however a limited experimental knowledge for these systems. The measurements of Hess *et al.*[14] indicate that Ne undergoes a wetting transition at a temperature within 2% of T_c on a Rb surface and that it undergoes a drying transition on Cs. Nonwetting of Ar on a Cs surface has been proposed on the basis of desorption experiments.[19] No experimental information is available at present on the wetting properties of Ar and Ne on other alkali surfaces.

In the absence of experimental observations, numerical simulations may play an important role in understanding the wetting properties of fluids and may be used as a useful guide in the choice of systems to be studied experimentally. We present in this paper one such calculation, based on a density-functional approach, where the adsorption properties of simple classical fluids (namely Ar and Ne) on Li and Na surfaces are studied. Ne on Rb has also been studied as a test case, where the wetting transition has experimentally been observed.[14] Recently, results of extensive Monte Carlo (MC) simulations on the Ne/Li system have been presented,[20] which seem to show that this system is nonwetting for all T between the triple point and the critical point. As shown in the following, our calculations predict quite a different scenario, and are in fact consistent with prewetting transitions below the critical point. We will discuss the discrepancies between our findings and the MC results of Ref. 20 in Sec. III.

II. COMPUTATIONAL METHOD

In recent years density-functional (DF) methods have become increasingly popular because of their ability to describe inhomogeneous fluids and phase equilibria. Comparison with simulation results shows that, once the long-range (van der Waals) attractive forces exerted by a surface on the gas atoms are included in the free energy density functional, the method provides a qualitatively (and most often quantitatively) good description of the thermodinamics of gas adsorption on a solid surface and in particular it is able to predict correctly a large variety of phase transitions (wetting, prewetting, layering, etc.).

In the density-functional approach the free energy of the fluid is usually written in terms of the density $\rho(\vec{r})$ of the fluid as: (for further details see Refs. 21–25)

$$F[\rho]=F_{HS}[\rho]+\frac{1}{2}\int\int \rho(\vec{r})\rho(\vec{r}')u_a(|\vec{r}-\vec{r}'|)d\vec{r}d\vec{r}' + \int \rho(\vec{r})V_s(\vec{r})d\vec{r}. \quad (1)$$

Here, F_{HS} is the free-energy functional for an inhomogeneous hard-sphere (HS) reference system, the second term is the usual mean-field approximation for the attractive part of the fluid-fluid intermolecular potential u_a,[26] while $V_s(\vec{r})$ is the external adsorption potential due to the surface. For F_{HS} we use the nonlocal functional of Ref. 27 written in terms of a suitable coarse-grained density obtained by averaging the true fluid density over an appropriate local volume. This scheme predicts good triplet correlation functions $c^{(3)}(\mathbf{r},\mathbf{r}')$ for a bulk one-component fluid. In addition, applied to liquid-solid interfaces, it gives fairly good results when compared to ''exact'' Monte-Carlo computer simulations, even in the presence of rapid oscillations of the liquid density such as those occurring in the close vicinity of the adsorbing surface.[27] For instance, both DF and MC simulations agree in predicting and locating the prewetting transitions in the case of Ar/CO_2 system.[29,30] As an even more stringent test, the two-dimensional limit of the theory of Ref. 27 has been studied:[28] the behavior of a three-dimensional (3D) DF theory in this limit is a good test of its performances for describing adsorption phenomena at low coverages. The overall agreement is surprisingly accurate.[28]

In order to include in this scheme correlation effects, which would be otherwise neglected in the mean-field treatment of the long-range attractive part of the adatom-adatom interaction appearing in the second term of Eq. (1), we follow Ref. 31 and regard u_a in Eq. (1) as an *effective* attractive interaction given by[31,32,30]

$$u_a(r)=0, \quad r\leqslant\lambda^{1/6}\tilde{\sigma} = 4\epsilon\{\lambda(\tilde{\sigma}/r)^{12}-(\tilde{\sigma}/r)^6\}, \quad r>\lambda^{1/6}\tilde{\sigma} \quad (2)$$

which for $\lambda=1$, corresponds to the bare attractive interaction. For $\lambda<1$ this effective potential has the same long-range properties as the bare interaction, which is an important factor when studying wetting phenomena, but its value at the minimum is increased by a factor λ^{-1}, to simulate qualitatively the above mentioned correlation effects. At any temperature, we treat the HS diameter $\tilde{\sigma}$ and the enhancing factor λ as free parameters determined by requiring that the experimental values of the liquid and vapor densities at coexistence, ρ_l and ρ_v, are reproduced for the bulk fluid, as explained in detail in the following section.

As for the interaction with the substrate, we make the usual approximation of treating it as an inert, planar surface acting on the the fluid as an external potential $V_s(z)$(z is the coordinate normal to the surface plane). Accurate *ab initio* potentials are now available,[33] which describe the interaction between noble gases and the alkali surfaces. Approximating the true surface by an ideal plane should not be a very bad approximation for these systems, given the uniformity and almost complete lack of corrugation of clean alkali surfaces. The equilibrium density profile $\rho(z)$ of the fluid adsorbed on the surface is determined by direct minimization of the functional in Eq. (1) with respect to density variations. In practice, at a given temperature, we fix the coverage $\Gamma=\int[\rho(z)-\rho_v]dz$ and solve iteratively the Euler equation $\mu=\delta F/\delta\rho(z)$ by using a fictitious dynamics, with the value of the chemical potential μ fixed by Γ. The results of such minimizations are reported and discussed in the following section.

TABLE I. Values of $\tilde{\sigma}/\sigma_{LJ}$ and λ used to obtain the agreement between the experimental and calculated values of coexistence densities for bulk Ar at the saturation pressure, as explained in the text. Calculated values are reported in parenthesis.

T(K)	P^*	ρ_v^*	ρ_l^*	$\tilde{\sigma}/\sigma_{LJ}$	λ
124	0.036 (0.037)	0.044 (0.044)	0.669 (0.669)	0.9562	0.5810
126	0.040 (0.041)	0.049 (0.048)	0.658 (0.658)	0.9545	0.5815
128	0.044 (0.046)	0.055 (0.054)	0.646 (0.646)	0.9520	0.5840
129	0.046 (0.047)	0.058 (0.057)	0.638 (0.638)	0.9526	0.5838
130	0.048 (0.050)	0.061 (0.060)	0.634 (0.634)	0.9508	0.5833
132	0.053 (0.055)	0.068 (0.067)	0.621 (0.621)	0.9485	0.5855
137	0.066 (0.070)	0.089 (0.087)	0.586 (0.586)	0.9438	0.5886
138	0.069 (0.073)	0.094 (0.092)	0.578 (0.578)	0.9428	0.5897
139	0.073 (0.077)	0.100 (0.098)	0.569 (0.569)	0.9416	0.5912
140	0.076 (0.081)	0.106 (0.103)	0.561 (0.560)	0.9404	0.5923

III. RESULTS AND DISCUSSION

Our results are based on the analysis of adsorption isotherms, calculated by using the DF described in the previous section, for the case of Ar and Ne adsorption on planar surfaces representing Li and Na surfaces, respectively.

The bare Ne-Ne and Ar-Ar interactions are usually given in the form of a Lenard-Jones (LJ) 12-6 potential, with parameters[34,20] $\epsilon_{Ne-Ne}/k=33.9$ K, $\sigma_{Ne-Ne}=2.78$ Å, and $\epsilon_{Ar-Ar}/k=119.8$ K, $\sigma_{Ar-Ar}=3.405$ Å.

We use in Eq. (2) the above values for ϵ, while we determine the two adjustable parameters entering the functional (1), i.e., the HS diameter $\tilde{\sigma}$ and the corrective factor to the potential well depth λ appearing in Eq. (2), by imposing that the experimental bulk phase diagram of the adsorbed fluid (either Ar or Ne) is correctly reproduced. In particular, it is crucial to verify that the choice of these two parameters leads to the correct thermodynamic equilibrium conditions. We have calculated several isotherms for a bulk system. If the temperature is lower than the critical temperature then a blip in the P-V plane, including region of positive slope, $(\partial P/\partial V)_T>0$, develops. As usual, the densities of the coexisting liquid and gas and the equilibrium pressure are found by applying a Maxwell (equal-area) construction in the P-V plane. For a particular choice of $\tilde{\sigma}$ and λ, this construction gives the vapor pressure P and the liquid and vapor densities ρ_v and ρ_l at a given temperature. At any T, we determine the parameters $\tilde{\sigma}$ and λ giving the best fit to the experimental values of $P(T)$, $\rho_v(T)$, and $\rho_l(T)$. A summary of our best fit parameters are given in Tables I and II, while our results for the coexistence line in the (ρ^*,P^*) plane are shown in Fig. 1 (we use reduced units for the quantities considered. These are defined as: $P^*=P\sigma_{LJ}^3/\epsilon$; $\rho^*=\rho\sigma_{LJ}^3$, where ϵ and σ_{LJ} are the Lenard-Jones parameters of the bare atom-atom interaction).

TABLE II. Same as in Table I, for bulk Ne.

T(K)	P^*	ρ_v^*	ρ_l^*	$\tilde{\sigma}/\sigma_{LJ}$	λ
39	0.058 (0.061)	0.074 (0.072)	0.596 (0.596)	0.9537	0.5526
40	0.067 (0.071)	0.088 (0.086)	0.574 (0.574)	0.9497	0.5536
41	0.077 (0.083)	0.106 (0.103)	0.549 (0.549)	0.9455	0.5549
42	0.089 (0.096)	0.127 (0.124)	0.520 (0.520)	0.9413	0.5567
43	0.102 (0.104)	0.156 (0.138)	0.482 (0.482)	0.9470	0.5503
44	0.116 (0.123)	0.206 (0.201)	0.417 (0.416)	0.9347	0.5695

We notice that the value of λ is such as to increase the depth of the effective potential u_a over the depth of the corresponding bare potential by a factor $\simeq 1.78$ for Ar and $\simeq 1.8$ for Ne. These values are of the same order of magnitude as that obtained in Ref. 32 by fitting T_c for Ar and are reasonable in order to describe the effect of the peak in the pair correlation function $g(r)$ at the intermediate densities of interest. A second comment refers to the fitted values of the $\tilde{\sigma}$'s, which turn out to be about 5% smaller than the LJ values quoted above, usually employed in Monte Carlo calculations.[20,32] As a consequence, the coefficients of the long-range attraction, $C_6=4\epsilon\tilde{\sigma}^6$ are reduced by about 30% with respect to the corresponding above mentioned LJ values, and are in a much better agreement with the most accurate theoretical values.[35] As remarked in Ref. 26, however, the LJ parameters have nothing of fundamentals and are only determined to provide reasonable agreement between ''exact'' results (say, from Monte Carlo simulations) and the experimental results in the bulk liquids. In other words, they are not the values that would apply to an isolated pair of Ar or Ne atoms. Similarly, our $\tilde{\sigma}$'s are fitted so that the values predicted by our DF calculation for the coexistence pressure at a given T and for the corresponding densities agree with their experimental counterparts. In view of this, our effective interaction entering Eq. (2) should not be regarded as a pair potential and we do not expect that, when inserted in a Monte Carlo simulation, it would necessarily lead to the same results as those found from our DF treatment.

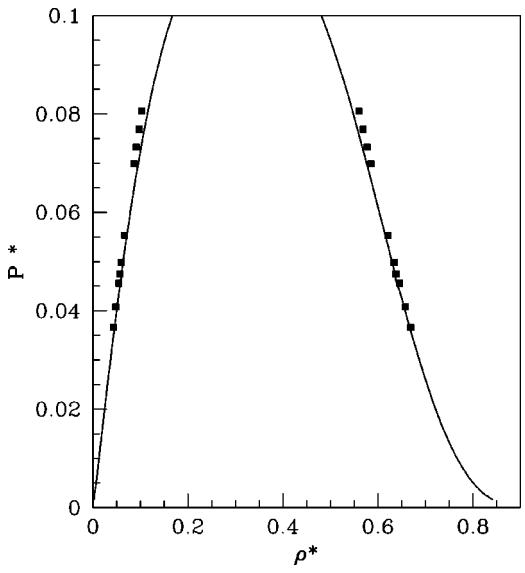

FIG. 1. Phase diagram of bulk Ar. Squares: calculated points. Solid line: experimental curve.

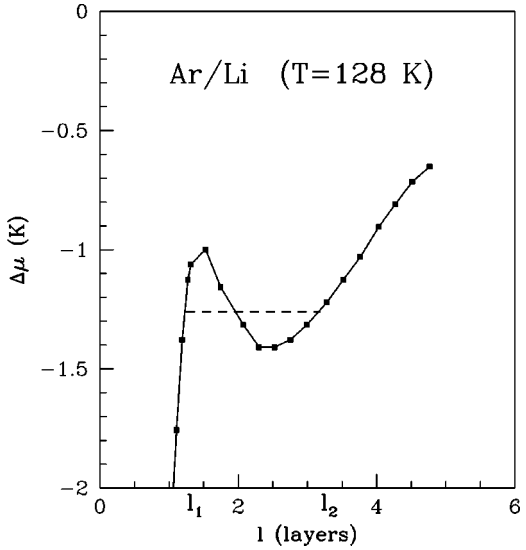

FIG. 2. Chemical potential (measured with respect to its value at bulk liquid-vapor coexistence) as a function of coverage for the Ar/Li system at $T=128$ K. The dashed line shows the value of $\Delta\mu$ satisfying the equal-area Maxwell construction: the thickness of the ''thin'' and ''thick'' film in equilibrium at this value are indicated on the x axis.

Once the bulk properties are optimized in the way described above, we switch on the adatom-surface potential in Eq. (1) and compute the chemical potential μ corresponding to the equilibrium density profile for a given coverage, as described in Sec. II. The coverage is expressed in nominal layers $l=\rho_l^{-2/3}\int_0^\infty[\rho(z)-\rho_v]dz$. The collection of pairs (μ,l) at equilibrium, at a given T, provides an adsorption isotherm. As an example the isotherm of Ar/Li at $T=128$ K is shown in Fig. 2, where the chemical potential, measured with respect to its value at coexistence, is plotted as a function of film thickness. For small coverages the chemical potential increases approaching the saturation value from below. For certain temperatures like the one considered in Fig. 2, however, a sudden change in slope is observed as the coverage is further increased. After reaching a minimum value, the chemical potential rises again, generating in the $\mu-l$ plane a van der Waals-like loop, as the one shown in Fig. 2. Since films for which μ has a negative slope are unstable, this structure reveals the existence of a first-order transition between films of different thickness. The amplitude of the transition (i.e., the amplitude of the discontinuous jump in coverage) is determined by making an equal-area Maxwell construction, as shown in Fig. 2 with a dashed line: two equilibrium thicknesses are thus identified, l_1 and l_2, and the jump between them corresponds to the prewetting transition.

A few equilibrium density profiles are shown in Fig. 3, for coverages smaller and larger, respectively, than the thin-thick film values l_1 and l_2 determined above.

We summarize our results for the Ar/Li system in Fig. 4, where the calculated adsorption isotherms for this system are shown for a number of temperatures. It appears from Fig. 4 that a wetting transition occurs at $T\simeq 124$ K, accompanied by first-order prewetting transitions at higher T. The ampli-

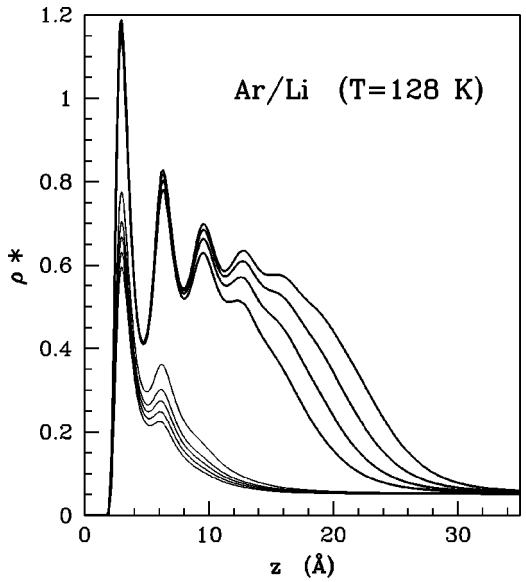

FIG. 3. Density profiles of Ar films on the Li surface, plotted as a function of the distance from the surface plane. The thin lines show the density profiles at coverages below the ''thin'' film thickness l_1 (see Fig. 2), the thicker lines show the density for film thickness larger than the value l_2 shown in Fig. 2. The origin of the z coordinates is taken at the surface plane position.

tude of the prewetting transition decreases with temperature, until it vanishes at a critical value $T_{pw}^c \simeq 130$ K. At temperatures higher than T_{pw}^c a continuous wetting of the surface takes place.

Seen in the $(\mu - T)$ plane the occurrence of these first-order wetting transitions is represented by a line leaving smoothly the liquid-gas coexistence curve at T_w and ending at the prewetting critical temperature T_{pw}^c. On general grounds one expects $\Delta\mu \equiv \mu - \mu_{coex} \sim -a(T - T_w)^{3/2}$, where the exponent 3/2 is related to the exponent of the van der Waals tail $-C_3/z^3$ of the surface potential. We show in Fig. 5 our calculated values for $\Delta\mu$, together with a fit with the expected analytical form.

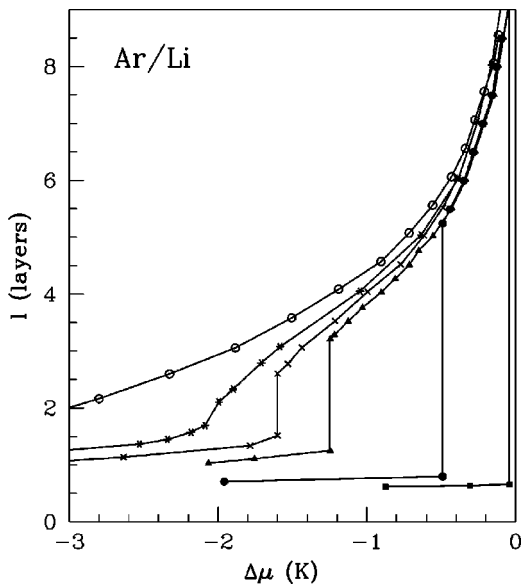

FIG. 4. Adsorption isotherms for the Ar/Li system. $\Delta\mu$ is measured from the saturation value. Squares: $T = 124$ K; Full dots: $T = 126$ K; Triangles: $T = 128$ K; Crosses: $T = 129$ K; Stars: $T = 130$ K; Open dots: $T = 132$ K.

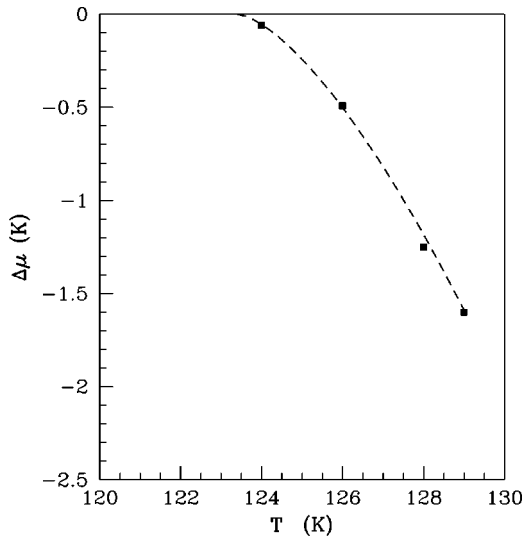

FIG. 5. Calculated wetting phase diagram for the Ar/Li system. The squares are the calculated points, the dashed line is a fit, as described in the text.

Figures 6, 7, and 8 show the calculated adsorption isotherms for Ar/Na, Ne/Li, and Ne/Na, respectively. In all cases a sequence of prewetting transitions is found, below the bulk critical temperature [T_c(Ar) = 150.9 K and T_c(Ne) = 44.4 K]. In Table III, we summarize the wetting and critical prewetting temperatures obtained from our calculated adsorption isotherms.

The last line in Table III refers to the system Ne/Rb experimentally investigated by Hess *et al.*[14] We calculated two isotherms for this system, at $T = 43$ K and $T = 44$ K. We find nonwetting behavior at $T = 43$ K, while at $T = 44$ K complete wetting occurs. We thus estimate $T_w \sim 44$ K for

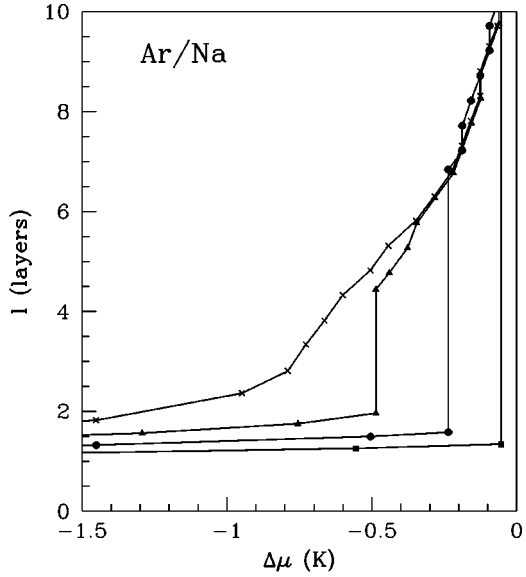

FIG. 6. Adsorption isotherms for the Ar/Na system. Squares: $T = 137$ K; Full dots: $T = 138$ K; Triangles: $T = 139$ K; Crosses: $T = 140$ K.

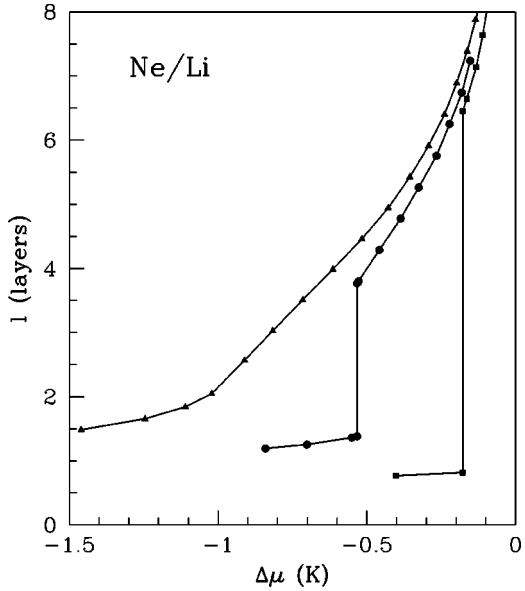

FIG. 7. Adsorption isotherms for the Ne/Li system. Squares: $T=39$ K; Full dots: $T=40$ K; Triangles: $T=41$ K.

this system, but we are not able to resolve any prewetting line of transitions between these two temperatures. Both the wetting temperature and the temperature interval $|T_w-T_{pw}^c| \sim 1$ K separating the nonwetting from the complete continuous wetting regimes are in excellent agreement with experiments.[14] Although the almost perfect agreement between theoretical and experimental values of T_w should be regarded as fortuitous in view of the many approximations contained in our calculations (planar surface, DF treatment, effective potential fit, etc.), nonetheless it is rewarding to find that our treatment correctly predicts the observed wetting transition.

A simple heuristic model has been proposed by Cheng *et al.*[36] where the energy cost of forming a thick film is compared with the benefit due to the gas-surface attractive interaction, resulting in an implicit equation for the wetting temperature

$$(\rho_l-\rho_v)\int_{z_0}^{\infty} V_s(z)dz=-2\gamma. \tag{3}$$

Here, ρ_l and ρ_v are the densities of the adsorbate liquid and vapor at coexistence, γ is the surface tension of the liquid and z_0 is the equilibrium distance of the gas-surface interaction potential V_s. If one inserts in Eq. (3) the potential V_s used in our calculations, and the experimental values for $\rho_l(T)$, $\rho_v(T)$, and $\gamma(T)$, values of the wetting temperature, T_w systematically lower than those found in our calculations are predicted, as shown in the column T_w^C of Table III. The apparent failure of this simple model to describe wetting behavior in the case of ultraweak potentials, such as those investigated here, has already been pointed out in Ref. 37, where extensive Monte Carlo calculations for systems exhibiting wetting at the triple point show that the simple criterion quoted above actually overestimate the wetting, insofar as it predicts a lower well depth threshold for triple-point wetting than the simulations find.

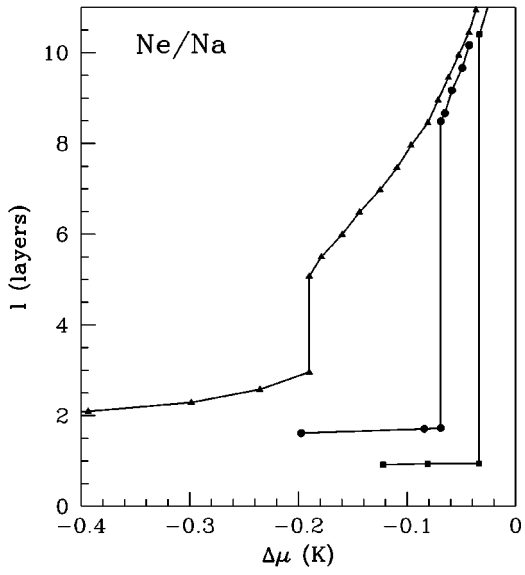

FIG. 8. Adsorption isotherms for the Ne/Na system. Squares: $T=41$ K; Full dots: $T=42$ K; Triangles: $T=43$ K.

TABLE III. Wetting (T_w) and critical prewetting (T_{pw}^c) temperatures from DF calculations. The column labeled T_w^C reports the prediction of Eq. (3).

Gas/Surface	T_w	T_{pw}^C	T_w^C	T_w^{expt}
Ar/Li	123 ($0.81\,T_c$)	130	107	
Ar/Na	136 ($0.90\,T_c$)	140	117	
Ne/Li	38 ($0.86\,T_c$)	41	33	
Ne/Na	40 ($0.90\,T_c$)	44	36	
Ne/Rb	44 ($0.99\,T_c$)	-	38	43

Prewetting transitions in classical fluids are notoriously elusive. On the basis of model calculations, it has been suggested[38] that one possible reason for this elusiveness is that they lie so close to the adsorbate bulk coexistence line as to render them difficult to detect. This happens because the adatom-substrate potential is comparable in strength with the adatom-adatom potential. The model calculations of Ref. 38 show that, for a wide range of interaction parameters, the prewetting line lies at a chemical potential, which differs from that of coexistence by an amount on the order of 10^{-3} KT_c. Our results show no exception to this behavior, although the proximity to coexistence, which makes prewetting transitions so difficult to observe experimentally, is slightly lower than expected. In the case of Ne/Li the values of the chemical potential for which we find discontinuities in coverage are only 1 K (at most) below the saturation value (see Fig. 7), while for Ar/Li they are 2 K (at most) below (see Fig. 4). Thus, $\Delta\mu \sim 10^{-2}$ KT_c. The vapor pressure at which the prewetting jumps should be observed for the system we have investigated, may then be approximately estimated by assuming ideal gas behavior for the vapor phase (see Ref. 20 for a better estimate). For $\Delta\mu \sim 2$ K, one finds $P=P_{sat}\ \exp(\Delta\mu/T) \sim 0.985 P_{sat}$, thus in a range that may be accessible to experiments.

We mention at this point recent results[20] based on extensive Monte Carlo simulations on the behavior of Ne on a Li

surface (the gas-surface potential used in these simulations is the same as used here) where nonwetting behavior up to the critical point has been found, at variance with the results presented here. One may invoke various explanations for these different findings. For example one could think that metastability in the region close to the critical point may affect seriously MC simulations and that reliable results may require a number of MC moves prohibitively large to reach the regime where the wetting transition is found.

Another possible explanation on why Bojan *et al.* do not see wetting of Ne on Li is that the prewetting regime is so close to saturation that their simulation cannot discern it. In fact at 40 K we find a prewetting jump of slightly more than two layers at a chemical potential only 0.5 K below saturation. At lower temperatures, where the jump is larger, it occurs even closer to saturation. The situation is even worse for Ne/Na. It seems to be more promising for Ar/Li, where one should see a $\sim 2-3$ layers jump ~ 1.5 K below saturation at $T=128$ K, so this is the system were we suggest to make experiments.

We remark at this point the extreme sensitivity of the results presented above to the details of the gas-surface interaction potential. It has been shown recently,[39] for the case of Ar/CO_2 system, that minor changes in the overall shape of the adsorption potential may alter dramatically the properties of the adsorbed film. In order to evaluate the sensitivity of the present results to the shape of the substrate potential, we recalculated the wetting diagram of Ar/Li by using a 9-3 Lenard-Jones potential to describe the Ar-surface interaction, instead than the *ab initio* potentials used above,[33] and adjusting the two parameters entering the 9-3 potential in order to have the same well depth D and minimum position as the *ab initio* potential. We found that the wetting temperature calculated with this interaction increases from 123 to 136 K, while the prewetting critical temperature changes from 130 to 138 K. This is not surprising, given the dependence of the wetting temperature, as is clear from the implicit definition Eq. (3), from the global shape of the potential, and not just from the well depth and position of the minimum.

Of course the wetting properties will also be very sensitive to the adatom-adatom potential which determines the surface tension explicitly entering Eq. (3). Thus, on these very weak substrates, wetting or nonwetting above the triple point, but below T_c, is the result of a delicate balance between adatom-substrate and adatom-adatom interactions. In view of this, we suggest another possible reason of the discrepancy between our findings and the MC results of Bojan *et al.*,[20] i.e., the different long-range behavior of our effective interaction u_a [see Eq. (2) and the ensuing discussion] and of the bare LJ potential used in the Monte Carlo simulations of Ref. 20. Experiments are currently in progress,[40] which will hopefully be able to verify the predictions contained in this paper.

ACKNOWLEDGMENTS

We thank G. Mistura, L. Bruschi, M. W. Cole, and S. Curtarolo for useful discussions and critical comments. We thank S. Curtarolo for sending us a copy of the manuscript[37] prior to publication.

[1] J. W. Cahn, J. Chem. Phys. **66**, 3667 (1977).

[2] P. Taborek and J. E. Rutledge, Phys. Rev. Lett. **68**, 2184 (1992); G. B. Hess, M. J. Sabatini, and M. H. W. Chan, *ibid.* **78**, 1793 (1997); D. Ross, P. Taborek, and J. E. Rutledge, Phys. Rev. B **58**, R4274 (1998); G. Mistura, H. C. Lee, and M. H. W. Chan, J. Low Temp. Phys. **96**, 1 (1994).

[3] H. Kellay, D. Bonn, and J. Meunier, Phys. Rev. Lett. **71**, 2607 (1993).

[4] V. F. Kozhevnikov, D. I. Arnold, S. P. Naurzakov, and M. E. Fisher, Phys. Rev. Lett. **78**, 1735 (1997).

[5] R. Lucht and C. Bahr, Phys. Rev. Lett. **78**, 3487 (1997).

[6] D. Beysens and D. Esteve, Phys. Rev. Lett. **54**, 2123 (1985).

[7] E. Cheng, M. W. Cole, W. F. Saam, and J. Treiner, Phys. Rev. Lett. **67**, 1007 (1991); Phys. Rev. B **46**, 13 967 (1992); **47**, 14 661(E) (1993).

[8] P.-J. Nacher and J. Dupont-Roc, Phys. Rev. Lett. **67**, 2966 (1991); P. J. Nacher, B. Demolder, and J. Dupont-Roc, Physica B **194**, 975 (1994).

[9] J. Rutledge and P. Taborek, Phys. Rev. Lett. **69**, 937 (1992); J. E. Rutledge and P. Taborek, J. Low Temp. Phys. **95**, 405 (1994); D. Ross, J. A. Phillips, and P. Taborek, *ibid.* **106**, 81 (1997); D. Reinelt, H. Gau, S. Herminghaus, and P. Leiderer, Czech. J. Phys. **46**, 431 (1996).

[10] K. S. Ketola, S. Wang, and R. B. Hallock, Phys. Rev. Lett. **68**, 201 (1992); R. B. Hallock, J. Low Temp. Phys. **101**, 31 (1995); A. F. G. Wyatt, J. Klier, and P. Stefanyi, Phys. Rev. Lett. **74**, 1151 (1995).

[11] E. Cheng, G. Mistura, H. C. Lee, M. H. W. Chan, M. W. Cole, C. Carraro, W. F. Saam, and F. Toigo, Phys. Rev. Lett. **70**, 1854 (1993).

[12] D. Ross, J. E. Rutledge, and P. Taborek, Fluid Phase Equilibria **150-151**, 599 (1998); Science **278**, 664 (1997); J. A. Phillips, P. Taborek, and J. E. Rutledge, J. Low Temp. Phys. **113**, 829 (1998); J. A. Phillips, D. Ross, P. Taborek, and J. E. Rutledge, Phys. Rev. B **58**, 3361 (1998); D. Ross, P. Taborek, and J. E. Rutledge, *ibid.* **58**, R4274 (1998).

[13] G. Mistura, H. C. Lee, and M. H. W. Chan, J. Low Temp. Phys. **96**, 221 (1994); D. Ross, P. Taborek, and J. E. Rutledge, Phys. Rev. B **58**, R4274 (1998).

[14] G. B. Hess, M. J. Sabatini, and M. H. W. Chan, Phys. Rev. Lett. **78**, 1739 (1997).

[15] F. Hensel and M. Yao, Eur. J. Solid State Inorg. Chem. **34**, 861 (1997).

[16] V. F. Kozhevnikov, D. I. Arnold, S. P. Naurzakov, and M. E. Fisher, Fluid Phase Equilibria **150-151**, 625 (1998).

[17] H. Nakanishi and M. E. Fisher, Phys. Rev. Lett. **49**, 1565 (1982).

[18] For reviews, see S. Dietrich, in *Phase Transitions and Critical Phenomena*, edited by C. Domb and J. L. Lebowitz (Academic, London, 1988), Vol. 12, p. 1; *Liquids at Interfaces*, edited by J. Charvollin *et al.* (North-Holland, Amsterdam, 1990), Courses 9, 10, and 11.

[19] W. Friess, T. Brunner, and D. Menzel, Surf. Sci. **309**, 182 (1994).

[20] M. J. Bojan, G. Stan, S. Curtarolo, W. A. Steele, and M. W. Cole, Phys. Rev. E **59**, 864 (1999).

[21] P. Tarazona, Mol. Phys. **52**, 81 (1984).
[22] T. F. Meister and D. M. Kroll, Phys. Rev. A **31**, 4055 (1985).
[23] S. Sokolowski and J. Fisher, Mol. Phys. **68**, 647 (1989).
[24] T. K. Vanderlick, L. E. Scriven, and H. T. Davis, J. Chem. Phys. **90**, 2422 (1989).
[25] D. M. Kroll and B. B. Laird, Phys. Rev. A **42**, 4806 (1990).
[26] M. P. Allen and D. J. Tildesley, *Computer Simulations of Liquids* (Clarendon Press, Oxford, 1990), p. 9.
[27] E. Kierlik and M. L. Rosinberg, Phys. Rev. A **42**, 3382 (1990).
[28] E. Kierlik and M. L. Rosinberg, Phys. Rev. A **44**, 5025 (1991).
[29] J. E. Finn and P. A. Monson, Phys. Rev. A **39**, 6402 (1989).
[30] Y. Fan and P. A. Monson, J. Chem. Phys. **99**, 6897 (1993).
[31] E. Velasco and P. Tarazona, J. Chem. Phys. **91**, 7916 (1989).
[32] E. Bruno, C. Caccamo, and P. Tarazona, Phys. Rev. A **35**, 1210 (1987).
[33] A. Chizmeshya, M. W. Cole, and E. Zaremba, J. Low Temp. Phys. **110**, 677 (1998).
[34] J. O. Hirschfelder, C. F. Curtiss, and R. B. Bird, *Molecular Theory of Gases and Liquids* (Wiley, New York, 1964).
[35] K. T. Tang and J. P. Toennies, Z. Phys. D **1**, 91 (1986).
[36] E. Cheng, M. W. Cole, W. F. Saam, and J. Treiner, Phys. Rev. B **48**, 18 214 (1993).
[37] S. Curtarolo, G. Stan, M. J. Bojan, M. W. Cole, and W. A. Steele, Phys. Rev. E (to be published).
[38] A. K. Sen and C. Ebner, Phys. Rev. B **33**, 5076 (1986).
[39] G. Mistura, F. Ancilotto, L. Bruschi, and F. Toigo, Phys. Rev. Lett. **82**, 795 (1999).
[40] G. Mistura and L. Bruschi (private communication).